General Disclaimer

One or more of the Following Statements may affect this Document

- This document has been reproduced from the best copy furnished by the organizational source. It is being released in the interest of making available as much information as possible.

- This document may contain data, which exceeds the sheet parameters. It was furnished in this condition by the organizational source and is the best copy available.

- This document may contain tone-on-tone or color graphs, charts and/or pictures, which have been reproduced in black and white.

- This document is paginated as submitted by the original source.

- Portions of this document are not fully legible due to the historical nature of some of the material. However, it is the best reproduction available from the original submission.

NASA CR-144502
ERIM 101800-20-F

Final Report

OIL POLLUTION DETECTION AND MONITORING FROM SPACE USING SKYLAB

GARY C. GOLDMAN AND ROBERT HORVATH
Infrared and Optics Division

NOVEMBER 1975

Prepared for

NATIONAL AERONAUTICS AND SPACE ADMINISTRATION

Johnson Space Center
Houston, Texas 77058
Contract No. NAS9-13281
Technical Monitor: L.B. York

ENVIRONMENTAL
RESEARCH INSTITUTE OF MICHIGAN
FORMERLY WILLOW RUN LABORATORIES, THE UNIVERSITY OF MICHIGAN
BOX 618 • ANN ARBOR • MICHIGAN 48107

TECHNICAL REPORT STANDARD TITLE PAGE

1. Report No.	2. Government Accession No.	3. Recipient's Catalog No.
101800-20-F		

4. Title and Subtitle	5. Report Date
OIL POLLUTION DETECTION AND MONITORING FROM SPACE USING SKYLAB	November 1975
	6. Performing Organization Code

7. Author(s)	8. Performing Organization Report No.
Gary C. Goldman and Robert Horvath	101800-20-F

9. Performing Organization Name and Address	10. Work Unit No.
Environmental Research Institute of Michigan Infrared and Optics Division Post Office Box 618 Ann Arbor, Michigan 48107	11. Contract or Grant No. NAS9-13281
	13. Type of Report and Period Covered Final Report
12. Sponsoring Agency Name and Address Lyndon B. Johnson Space Center National Aeronautics and Space Administration Houston, Texas 77058	14. Sponsoring Agency Code

15. Supplementary Notes

Technical Monitor was L. B. York

16. Abstract

The purpose of this report is to assess the feasibility of using satellite data as a means of monitoring and detecting oil spills on oceanic and estuarian waters.

One suspected spill was investigated using photointerpretation and digital-computer techniques on Skylab S190B and S192 data (Chapters 3 and 4). Other analysis techniques are also discussed (Chapter 5).

Indications are that any of these techniques might be usable if the spill is large enough to be seen by satellite, if the spill occurs more than a few kilometers offshore, if the sky and water are relatively clear, and if the data quality is good enough to see the small reflectance changes caused by the presence of the oil. In the case described in this report, the presence of the suspected spill could not be verified by computer techniques.

Although the Skylab program was not successful in demonstrating its feasibility for monitoring oil pollution, it did point out many of the drawbacks and operational problems that may be encountered. Monitoring and detecting oil spills could involve the integration of a satellite into a total surveillance scheme, if these drawbacks were corrected (Chapter 6).

17. Key Words		18. Distribution Statement
Oil spills	Satellite monitoring	Initial distribution is listed at the end of this document.
Oil slicks		
Oil pollution	Satellite detection	
Oceanic oil spills		
Estuarian oil spills	Skylab	

19. Security Classif. (of this report)	20. Security Classif. (of this page)	21. No. of Pages	22. Price
UNCLASSIFIED	UNCLASSIFIED	48	

PREFACE

The necessity of detecting and monitoring an increasing number of coastal oil spills has precipitated an increase in the evaluation of various surveillance methods.

The purpose of this study was to determine and demonstrate the present and future utility of space-acquired remote sensor data as an aid to the Coast Guard in fulfilling its assigned mission in the area of oil pollution detection and monitoring and law enforcement by specifically evaluating Skylab capabilities.

Various digital-computer and photointerpretation methods were attempted in order to develop, or at least evaluate, the best means of analyzing Skylab data.

This work was done under Contract NAS9-13281 for the National Aeronautics and Space Administration. We wish to thank the project monitor, L. B. York for his assistance in this state-of-the-art study.

ERIM personnel who contributed to this project were Drew Urbassik, Diana L. Rebel, Norman E.G. Roller, David R. Lyzenga, and Chester T. Wezernak, all of whom were of great technical and moral assistance. The work was performed in the Infrared and Optics Division under the direction of Richard R. Legault; Robert Horvath was Principal Investigator.

SUMMARY

The purpose of this study was to evaluate the feasibility of using satellite information as a means of detecting and monitoring oil spills.

Various digital-computer and photointerpretation techniques were used or considered on one suspected spill location, in the Gulf of Mexico.

The conclusions of the study and this report are as follows:

(1) Oil spills may be detected from space provided the following conditions exist: clear sky over the slick, relatively clear water, a spill more than a few kilometers from land, and a spill at least hundreds of meters long.

(2) Nearshore, coastal, bay, harbor, or river spills are very difficult to identify - but might possibly be detected.

(3) Positive detection or identification of a photographically (S190B) detected spill was impossible using the Skylab S192 (X-5 Array) data.

(4) A satellite detecting and monitoring system may be integrated into an overall surveillance program, but it must have daily visibility, high resolution, and many narrow spectral channels if it is to be successful in monitoring and detecting of oil spills.

CONTENTS

FIGURES

TABLES

1
INTRODUCTION AND SUMMARY

Petroleum products are becoming more commonly encountered as pollutants of our coastal and inland waters. These products result from natural seepage from the earth, accidental loss from equipment that is processing or using oil, deliberate dumping of oil waste from ships and coastal processing plants, or — even more frequently in recent times — from collision of oil tankers or other ocean-going ships. A timely detection method is necessary to enforce regulatory laws regarding oceanic dumping, to detect unreported spills so that financial liability can be assigned, and to assist clean-up measures to prevent ecological, aesthetic, or financial damage and loss.

Improvements in aerial and satellite instrumentation and data-processing techniques now provide another method of monitoring and detecting oil over large areas of water. Specifically, advances in multispectral sensing by remote means have increased the possibility for detection and identification of oil spills. With the presence of the Skylab satellite, scanning areas of coastal waters, observation and monitoring may now be considered using both satellite and conventional methods together.

The overall objective of this investigation was to determine and demonstrate the present and future utility of space-acquired remote sensor data as an aid to the Coast Guard in fulfilling its assigned mission in the area of oil-pollution detection and monitoring and law enforcement.

The purpose of this report is to use Skylab data to confirm, or at least investigate the feasibility of monitoring and detecting oil spills from space. An attempt is made to define oil-spill-signature

techniques. Finally, a brief evaluation of the Skylab program is made with respect to oil-spill detection, with a final evaluation of the utility of any space system for such a purpose.

During the course of this study, one suspected oil spill was investigated. Skylab data were processed for an area thought to have a high probability of seeping oil — the Gulf of Mexico, off the Louisiana coast. Although oil was detected here on the photographic imagery, multispectral scanner confirmation could not be made. However, an analysis of data quality was made, and various other digital-computer techniques, applicable to data of a higher quality than was obtained from Skylab, are discussed.

The last portion of this study is devoted to the evaluation of the Skylab sensors for potential use as a satellite monitoring and detection system for oil slicks. Evaluation is made as to the frequency of overflights, the acceptability of the detectors and their given channel bandwidths, and the usability and quality of the data, considering its clarity and background noise.

Appendix A contains a listing of all reported major oil spills occurring during the life of the satellite, along with the coincidence of the satellite's overflights.

2
THEORY AND INSTRUMENTATION

This chapter is devoted to a brief description of optical properties of oil and water as seen from space, Skylab instrumentation, some general radiation (visible and infrared) detector difficulties, and the constraints on using Skylab as a detector and monitor of oil spills.

2.1 OPTICAL PROPERTIES OF OIL ON WATER

The optical properties of oil, water and the oil-water interface of most interest to this study are specular reflectance, diffuse reflectance, extinction coefficient, index of refraction, and sacttering coefficient. These properties are discussed in References [1,2,3,4, and 5].

A summary of all the effects on the total reflectance of water, and oil on water, is that the specularly reflected component of the radiance from the oil slick will always be larger than that from water of similar surface roughness. This will exist regardless of sea state or illumination level (except in the case of whitecaps). However, the slick may sufficiently reduce the capillary waves present so that the otherwise present glitter pattern is subdued within the slick boundaries. In the case of diffuse reflectance (at least in the spectral region of our concern), the diffuse reflectance of natural water exceeds that of oil slicks. The slick tends to reduce the effective diffuse reflectance both by absorbing the downwelling energy (from the sky and sun) before it reaches the water, and by absorbing the upwelling energy after it leaves the water. Thus, the diffuse reflectance of a thicker oil slick on water will be less than

that of a thinner one. The relative magnitude of the two components of reflectance (diffuse and specular) from a target is, therefore, a function of the oil thickness, the solar-elevation angle (the angle of the sun above the horizon), the total solar illumination, the sea state, and the type of oil. It is impossible, therefore, to generalize the relative target reflectance of an oil slick on water as being more or less bright in appearance than water alone.

An example of this inability to predict relative total reflectance is seen next. The thickest portion of the oil slick is often located at or near the center of the slick. This center core may be darker (lower reflectance) than the surrounding water, if it is thick enough to seriously inhibit the diffuse upwelling radiation from the water. The upwelling may be the major component of the reflected energy in turbid water. Or, the core may be brighter than the surrounding water, if the water is dark-colored and specular reflectance is dominant — oil always has a higher specular reflectance than water. It is this apparent paradox that makes identification of oil spills difficult without adequate ground data to support the remote sensing.

To this inconclusiveness as to the relative brightness of the center portion of the oil in relation to the surrounding water, we must add the following complicating conditions. Natural water, sea or fresh, has extremely low reflectivity, about 2-10%. This results in extremely low-magnitude signals from the sensors on the satellite detectors. In some cases, in fact, the random electronic noise may generate signals higher in magnitude than those of the water or the oil. Therefore, it is sometimes necessary to measure variations of the very small target signal superimposed on a larger noise signal. This produces ambiguous results.

Another difficulty in assessing the characteristics (or even achieving positive identification) of oil floating on water is the possible presence of suspended particulate matter or plankton in the water. This will increase the reflectivity of the water (diffuse component) and overshadow the presence of oil. Correcting for this effect may include looking at the output signal from different spectral channels at the same time. Some channels are very sensitive to chlorophyll (phytoplankton) and some are sensitive to suspended particulate matter. But in almost all cases of all channels for moderate-thickness films, the reflectivity of at least the thin portions of oil on water should be uniformly higher than that of water alone. Techniques of ratioing total radiance values from one channel to another can help separate these effects and may confirm (or at least strongly suggest) the presence or absence of oil.

2.2 SKYLAB INSTRUMENTATION

The purpose of this brief description of the Skylab satellite instrumentation package is to give the reader some background to allow a more thorough understanding of some of the procedures and solutions discussed later.

We are concerned here with three instruments: (1) the S190A Multispectral-Photographic Camera; (2) the S190B Earth-Terrain Camera; and (3) the S192 Multispectral Scanner.

The S190A system was used to obtain multispectral photography by using various 70 mm film/filter combinations. The sensor consisted of six bore-sighted, high-precision f/2.8, 21.2° field-of-view lenses. This resulted in coverage of a 163 km^2 area and a scale of 1:3,000,000. The camera could simultaneously look at the same earth position with six spectrally sensitive films; two black and white films, sensitive

to the infrared; one color film, sensitive to the infrared; two black and white films, sensitive to visible light; and one high resolution color film, sensitive to the entire visible spectrum. This latter product was used in this study, giving a ground resolution of 24 m.

The S190B system was used to obtain high resolution images of small areas within the fields-of-view of the other instruments, to aid in their interpretation. This system used a camera with a 114 mm (4.5 in) format film and an f/4, 46 cm focal-length lens. The resultant coverage was a 109 km^2 area with a ground resolution of better than 16 m and a contact scale of 1:936,000. Three types of film were used with this camera: aerial black and white, color infrared, and high-resolution color. The latter product was used during this study to search for possible anomalies caused by oil spills.

The S192 was expected to be the most useful tool from the Skylab mission concerning the needs of this investigation. The system could gather high-spectral resolution, quantitative line scan digital data from radiation reflected or emitted from a portion of the earth's surface using 13 spectral intervals from 0.41 to 12.5 μm. Table 1 gives the spectral coverage and approximate sensitivities for each of these spectral channels. The total viewing area seen by the S192 is 68.5 km wide (after the curvature of the scanning system is corrected); the instantaneous field of view is about 80 x 80 m. The final S192 output (on computer-compatible magnetic tape) from each spectral channel (after noise removal, line straightening, and range adjustment) is in quantized steps from 0-255 counts.

TABLE 1. SKYLAB S192 MULTISPECTRAL SCANNER CHANNELS

SDO CHANNEL	SPECTRAL LIMITS (μm)	RADIANCE/COUNT ($\mu W/cm^2 sr$)
22	0.41-0.46	--
18	0.46-0.51	--
1 & 2	0.52-0.56	--
3 & 4	0.56-0.61	16.2
5 & 6	0.62-0.67	--
7 & 8	0.68-0.76	41.4
9 & 10	0.78-0.88	79.2
19	0.98-1.08	36.9
20	1.09-1.19	31.4
17	1.20-1.30	--
11 & 12	1.55-1.75	32.2
13 & 14	2.10-2.35	10.3
15, 16 & 21	10.20-12.50	38.6

The biggest problem seen in the data was the large magnitude of the electronic noise, especially for the visible and near-infrared channels of SL-4 (the X-5 array is discussed in Appendix A). This was a result of a last minute change in the detector package, which gave better quality to the thermal (infrared) channels at the expense of the others. An analysis of the noise problem is given in Section 3, but may be briefly summarized here by saying that over an apparently uniform area of the earth (clear water) the standard deviation for each channel output varied from 25% to 200% of the mean for that channel. This variance is too high to detect the small changes effected by the presence of oil.

2.3 RADIATION SOURCES FOR SATELLITE SCANNERS

There are many sources of radiant energy (both useful and not useful) seen by the satellites. The multispectral scanner can detect and quantify radiant energy within the wavelength limits of 0.4 to 12.5 μm. Within these limits, energy received from the sun and sky is specularly and diffusely reflected from the target (spot on the earth that the optics are looking at). The optics also receive scattered radiation from clouds, atmospheric particulate matter, and areas on the earth's surface near the target.

Of these various energy sources, the specularly and diffusely reflected radiation carries the most information (except for the 10.2 to 12.5 μm channel). This radiation helps identify the target as to material and condition of material. It is this information that is used to interpret ground targets by remote sensing.

The other energy sources serve to raise the background and noise level of the output and mask small changes in the target material (or reflectivity).

Along with these undesirable energy sources, the condition of the earth's atmosphere must be taken into account. The atmosphere both absorbs energy (decreasing useful information from the target), scatters energy (both into the optical path from extraneous sources and out of the path from the target), and to a smaller degree, re-emits energy.

All these negative effects are dependent on (1) the zenith angle of the sun (length of atmosphere through which the sunlight must travel), (2) the angles between the sun, the target, and the satellite, (3) the wavelength of the radiant energy, and (4) the atmospheric state.

For interpretation of oil-water situations, most of these negative effects arise. The solar-zenith angle and the angles between the sun, the target, and the satellite must be considered to minimize the effects of atmosphere and of sun glint off the wave surfaces. Clouds and haze may cause scattering effects that overshadow the very low oil/water reflectances, especially for rivers or turbid coastal waters.

3
SKYLAB ANALYSIS AND RESULTS

This chapter discusses the analysis and results of the Skylab data.

3.1 COINCIDENCE WITH KNOWN SPILLS

Continuous investigation of the USCG and EPA pollution reports produced about 70 major spills during the lifetime of the Skylab flight program (Appendix B). All of these events were compared with the Skylab data files and failed to produce even one event with time-coincident coverage by Skylab sensors. It was therefore decided to undertake reconnaissance interpretation of the high-resolution S190B color photography in an attempt to locate unreported oil slicks. All S190B coverage of the Gulf of Mexico and the California coast was reviewed for this purpose. These areas were chosen as being most likely to contain oil slicks (from natural seeps, leaks from drilling operations, etc.). One frame of data was found to contain a slick-like anomaly, and S192 multispectral scanner data tapes for this area were ordered for detailed analysis.

The area selected was in the Gulf of Mexico, south of Atchafalaya Bay, about 30 km off-shore. This area was covered by Skylab-4 during pass 96 on 30 January 1974 from 16:55:07 to 16:55:21 hours. The scene is fairly clear, with clouds to the southeast and highly turbid water to the north (Figure 1).

3.2 DATA ANALYSIS

Three methods of data analysis were used on this data set. The first involved photointerpretation, using the S190A and the S190B

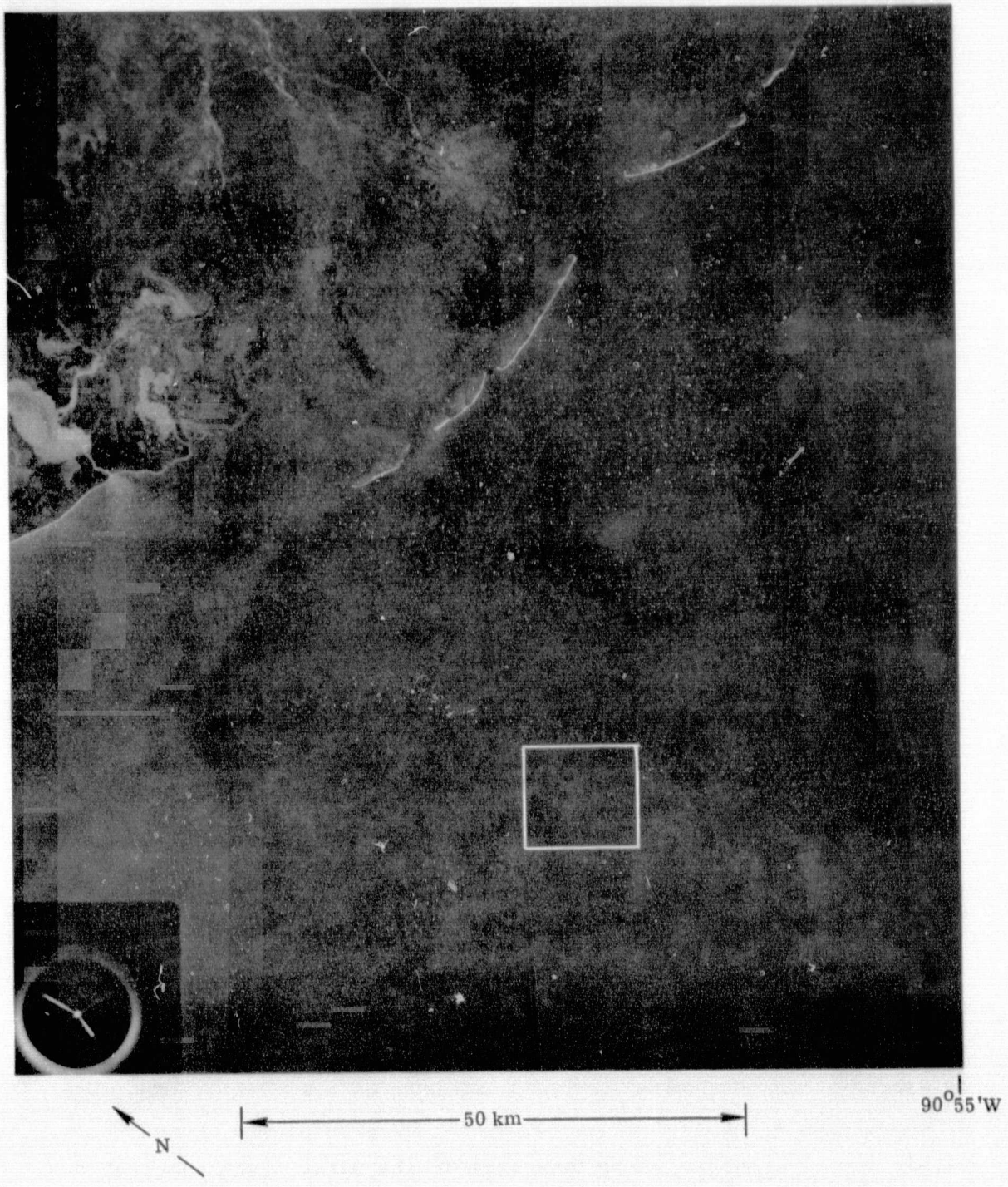

S190B Photography Collected on 30 January 1974 at 1655 hs GMT
(Roll #94, Frame #183)

FIGURE 1. LOCATION OF THE SUSPECTED SPILL IN THE GULF OF MEXICO

photographs. The second was a statistical analysis of the data quality for the magnetic tape products of the S192, in order to predict the best spectral channels to use based on data quality and availability. The third method involved summing the data values for two to four of the spectral channels to minimize the background and electronic noise.

3.2.1 PHOTOINTERPRETATION

Photographic analysis was carried out on a scale of 1:250,000 and less. The area was carefully observed on the high resolution S190B photography in an attempt to isolate possible occurrances of oil on the water. Many bright spots were visible, indicating the presence of oil drilling towers. Some larger areas of high brightness were speculated to be ships, and the visibility of their wakes usually confirmed this. At least one area (0.2-0.4 km^2) was highly suspected of being a possible oil seepage or spill.

The resolution and quality of these film products are excellent, so the above identifications were not impaired.

An attempt was also made to confirm the presence of the possible spill on the S190A. However, only the aerial color product was available, and it did not aid further in the investigation.

3.2.2 STATISTICAL ANALYSIS

A statistical analysis of data noise (by channel) was made before any other method of analysis was used on these data. An area covering about 20 x 30 km (about 85,000 pixels) was chosen within the clear-water, cloudless area of the data. Each spectral channel was evaluated separately to determine the mean data value, the range of values, and the standard deviation from the mean.

Table 2 shows the results of this analysis. In cases where more than one SDO channel covered the same spectral region, the channel with the best statistics was used.

The first notable feature of the table is the lack of data for five of the spectral channels. These data were not received with the others. The next feature is seen in the column labeled "Range". This column has the range of values for the given channel, after the end points of 0 and 255 have been eliminated. This elimination was made to try to overcome the extreme cases of either negative zero offset, clipping, or noise. The range of values for the reflective channels (not including SDO-15) varied from 55 to 167 data counts.

Another feature is seen in the column labeled "Good Points," which has the percentage of the 85,000 points remaining in each channel, after the end points (0 and 255) are eliminated. Of these points, only those "Good" for all eight usable channels simultaneously (7540 points) were included in the subsequent analysis for the mean and standard deviation. This qualification should bias the analysis toward the best case.

The main features of the columns headed "Mean" and "Standard Deviation" are the high values of the ratio of the standard deviation to the mean. This ratio varied from 28% to 111% in the reflective channels.

The last column, "NE(ΔCount)", shows the calculated standard deviation for the data noise, in units of counts, based on NEΔρ values furnished by NASA [6] for the X-5 detector array and a standard atmosphere model [7]. The noteworthy features of these values are their high count values, and their closeness in magnitude to the standard deviations

TABLE 2. RESULTS OF STATISTICAL ANALYSIS OF SKYLAB DATA QUALITY
(Data Values are in Counts, Rounded to the Nearest Whole Number)

SDO Channel	Wavelength (μm)	Good Points (%)	Range (Counts)	Mean (Counts)	Standard Deviation (Counts)	NE(ΔCount) (Counts)
22	0.41-0.46	NO DATA RECEIVED				
18	0.46-0.51	NO DATA RECEIVED				
1,2	0.52-0.56	NO DATA RECEIVED				
3	0.56-0.61	99	21-188	84	24	18
5,6	0.62-0.67	NO DATA RECEIVED				
7	0.68-0.76	91	1-82	19	10	9
9	0.78-0.88	87	1-63	11	5	5
19	0.98-1.08	74	1-191	13	14	10
20	1.09-1.19	64	1-96	9	10	9
17	1.2-1.3	NO DATA RECEIVED				
12	1.55-1.75	66	1-63	7	3	4
13	2.10-2.35	77	1-56	10	6	6
15	10.2-12.5	99+	87-118	98	4	

calculated over our near-uniform area. This helps confirm our conclusion that the observed variances represent data noise and not scene variability.

Again, it should be mentioned that this analysis was over a near-uniform reflecting area. Obviously, any hope of "seeing" small reflective anomalies due to the presence of oil is impossible by single-channel analysis with data of this quality.

3.2.3 RADIANCE SUMMATION

In an effort to minimize noise problems, individual channels and their spatially-coherent weighted sums were evaluated over the anomalous area discussed in Section 3.2.1, as seen on the S190B photograph.

The total area considered for this evaluation is 2.4 x 1.6 km, covering a total of about 600 pixels. Being well within the perimeter of the previously discussed uniform area, it was not surprising that the statistics for the four spectral channels chosen for evaluation (SDO-3, 7, 9, and 15) were nearly identical to those of the larger area.

The value of the data counts were printed for each of the above channels separately, as well as for the following weighted sums:

$$(1) \quad (\text{SDO-3}) + \frac{S_3}{S_7} (\text{SDO-7})$$

$$(2) \quad (\text{SDO-3}) + \frac{S_3}{S_7} (\text{SDO-7}) + \frac{S_3}{S_9} (\text{SDO-9})$$

$$(3)\quad \frac{S_3}{S_7}(SDO\text{-}7) + \frac{S_3}{S_9}(SDO\text{-}9)$$

$$(4)\quad (SDO\text{-}3) + \frac{S_3}{S_7}(SDO\text{-}7) + \frac{S_3}{S_9}(SDO\text{-}9) + \frac{S_3}{S_{15}}(SDO\text{-}15)$$

$$(5)\quad (SDO\text{-}3) + \frac{S_3}{S_7}(SDO\text{-}7) + \frac{S_3}{S_9}(SDO\text{-}9) - \frac{S_3}{S_{15}}(SDO\text{-}15)$$

where S_i is the standard deviation for channel "i". The weighted summation using ratios of the standard deviations was done to equalize the noise contribution of all the channels used in the summation.

Those values of sums falling within the highest 10% and those within the lowest 10% of the range were separated out as "special." In all cases, the location of these special values appeared random throughout the 600 pixel area. An example of this is seen in Figure 2. This figure shows the full 20 x 30 pixel area for channel SDO-7. The pixels having values in the upper 10% of the range for that channel are blacked out. There appears to be no apparent pattern. This lack of pattern is seen for all the four channels and the indicated sums. The area of the suspected spill is about 30-70 adjacent pixels in size. Therefore, if the data quality were of a high enough standard, some of this spot should be easily seen, and should be approximately in the center of Figure 2.

030 024 011 000 017 024 020 020 004 021 017 011 011 014 007 ■ 011 ■ 025 010 016 016 018 022 023 016 019 ■ 026 011 017
008 013 011 000 030 012 020 016 014 015 ■ 026 003 011 020 026 008 019 013 ■ 006 013 007 029 024 010 008 022 000 028 011
005 012 026 013 010 008 012 ■ 000 ■ 019 021 015 007 023 023 014 020 017 019 ■ 009 003 026 ■ 011 014 014 008 019 019
008 022 023 000 020 012 022 006 022 022 000 016 016 021 017 015 025 006 000 022 011 ■ 002 021 025 018 002 019 018 024 029
■ ■ 000 007 019 008 012 006 012 017 000 014 ■ 015 007 010 026 010 026 012 ■ 016 000 024 015 022 012 005 ■ 018 017
013 026 014 030 ■ 025 ■ ■ ■ 021 030 ■ 000 014 008 024 026 014 004 000 028 011 ■ 025 029 ■ 003 028 014 030 008
027 017 000 000 005 010 015 022 000 001 003 014 007 003 005 022 012 018 016 010 026 023 024 029 016 013 008 019 023 014 002
024 026 013 005 025 020 025 011 016 017 ■ 011 000 ■ 006 007 ■ 015 005 018 010 023 008 005 022 025 028 001 010 000 008
000 019 020 007 016 009 004 009 023 016 023 000 022 029 010 014 ■ 005 014 007 ■ 016 011 014 018 006 013 019 009 015 022
010 017 015 020 014 020 000 015 003 018 020 013 000 022 006 021 ■ ■ 027 005 013 028 017 009 030 ■ 022 010 ■ 020 005
008 029 023 023 012 004 000 023 010 027 015 013 027 008 000 000 022 028 014 000 024 009 015 022 019 007 014 021 019 004 015
007 013 011 018 013 013 ■ 028 013 025 012 001 023 020 010 008 ■ 021 005 003 ■ 018 025 015 003 ■ 019 010 012 015 022
027 016 ■ 000 018 019 017 ■ 022 021 019 019 005 009 014 000 022 020 000 ■ 006 018 010 029 000 007 000 014 022 011 013
014 002 024 024 018 012 027 018 000 006 012 022 012 022 007 007 007 003 006 011 021 018 006 011 017 026 013 008 014 030 019
013 010 006 015 005 ■ 012 ■ 006 023 007 010 020 004 004 016 012 ■ 020 001 022 022 018 011 015 021 024 000 000 021 002
027 022 025 ■ 007 028 007 026 000 029 022 ■ 023 021 019 ■ 009 002 005 014 002 026 014 011 016 021 021 ■ 007 026 017
■ 012 010 017 030 025 026 019 029 012 009 024 023 011 024 015 011 017 ■ ■ ■ 000 008 009 015 014 007 ■ 002 028 028
000 019 010 021 021 015 014 006 012 000 012 012 015 019 011 023 000 000 011 006 008 005 021 011 021 020 024 015 011 024 022
017 000 013 021 027 009 020 006 000 028 033 007 022 ■ 015 021 000 027 016 024 026 012 011 ■ 026 014 023 012 017 023 021
003 015 ■ 011 025 016 000 019 008 028 ■ 006 018 028 004 ■ 023 018 013 007 026 010 ■ 002 028 003 020 006 018 019 016

FIGURE 2. DIGITAL PRINTOUT OF SKYLAB CHANNEL SDO-7 COVERING THE AREA SUSPECTED OF AN OIL SPILL.
(The pixels blackened out have radiance values in the highest 10% of the range for that channel.)

An estimate of the degree of randomness of the data is seen by choosing any 100 (10 x 10) pixels. The mean number of either high or low special values should be 10 for a perfect infinite random set (10% of 100 pixels is 10 pixels). The actual value of the mean was about 10 (the value was not exactly 10 due to the quantization of the data and the finite sampling), and the standard deviation of the number of special values found over six areas, for each of the nine cases, is 3. The range of the number of special values for all these cases of 100-pixel sets was 4-16, or the mean plus or minus twice the standard deviation. Never were more than three or four adjacent pixels classified as "special." In many cases (about 30%) the special high values were immediately adjacent to the special low values.

Our sought-after oil spill was never discernible within the capabilities of the digital data, due to the excessive noise.

3.3 SKYLAB RESULTS

In summary, the following results can be stated regarding the Skylab analysis. The Skylab photography appears excellent, and one probable oil slick was detected in the S190B data. It was impossible to detect or identify this spill using the other data products. The sensor package for Skylab-4's S192 multispectral scanner, the X-5 array, had insufficient signal to noise ratio for this application so that any interpretation for this study was impossible.

4
OTHER METHODS OF ANALYSIS

This chapter is devoted to describing other methods of analysis using computer-compatible tape products of the S192 multispectral scanner that would have been used had the data been of higher quality. Along with the descriptions of these methods, a description of their resulting products will be given, as well as some examples, where applicable.

4.1 METHOD OF SPECTRAL SIGNATURES

If a spill is located under conditions of both clear sky and clean water, a suggested method of analysis is to attempt to derive spectral signatures by statistical means. This method will aid in comparing the signature with other known oil types and is also valuable where no ground data is available. The general procedure is to statistically identify as many different regions within the spill as possible, combine those regions whose signatures (reflected radiance values for each spectral channel) are nearly identical, and then compare this to signatures of known materials.

The first step in such an analysis may be to smooth out the random fluctuations in the data caused by either electronic or sensor noise. This smoothing may be done in a variety of ways, most of which simply involve averaging over a multi-pixel area, and redefining the pixel radiance value as being that average. This procedure is continued throughout the entire portion of the scene being analyzed. Obviously, the spatial extent of the features being analyzed must be significantly larger than the size of the multi-pixel area chosen for smoothing.

The next step in the process of calculating spectral signatures is to identify as many spectral classes in the scene as possible, and then find the radiance value, for each spectral channel, for all the pixels within each class. Finally, their mean and standard deviations are computed. The average mean value of radiance for each channel, together with the standard deviation from the mean for all pixels within the same target class make up the spectral signature for that class. Because a large number of signatures may be generated initially (due to the slight variations between classes), classes are usually grouped together if the values of their means for all the channels are relatively close.

There may be many products resulting from this method. Some of these are: (1) a recognition map showing the location of each of the target classes; (2) the listing of the means and standard deviations for each channel for each of the target classes; (3) the comparison of the different signatures for each of the classes.

An example of a recognition map is shown in Figure 3. This map displays target classes for an oceanic spill seen from ERTS-1 [8]. The brighter areas of the map are areas of relatively higher reflectance, while the darker indicate lower reflectance. It should be recalled that for this description, all spectral channels are compared simultaneously. One noteworthy feature of this particular recognition map is the brighter area near the center of the spill.

A visual display of the second product, the listing of the values of the means and standard deviations from the mean for each of the signature classes, may be seen in Figure 4. In this figure, also taken from the ERTS-1 study [8], the values for the means for three different signatured classes are displayed relative to the mean water values, for four spectral channels. Using a display such as Figure 4,

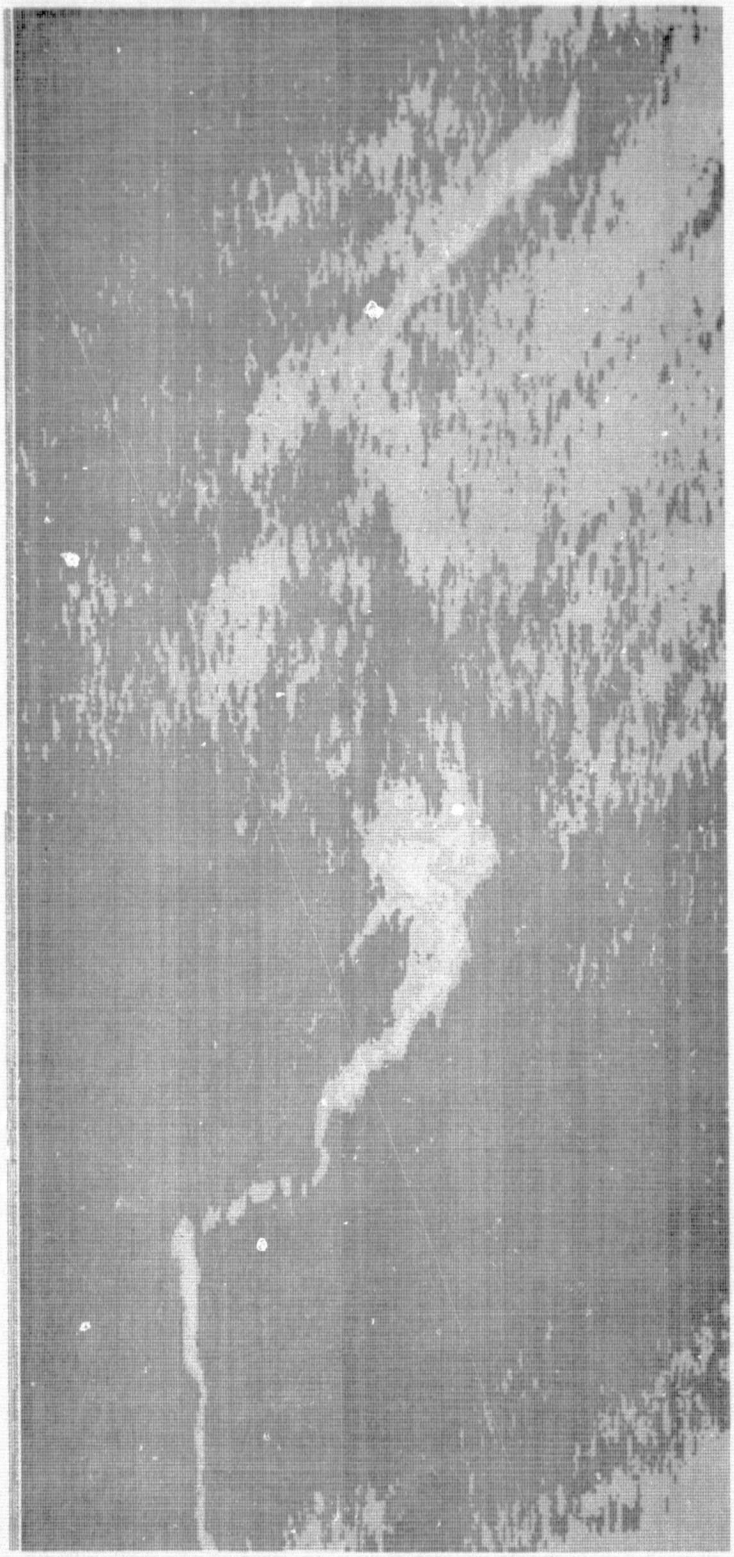

FIGURE 3. EXAMPLE OF SPECTRAL-SIGNATURE RECOGNITION MAP FOR AN OCEANIC SPILL.
From an ERTS-1 study [8].

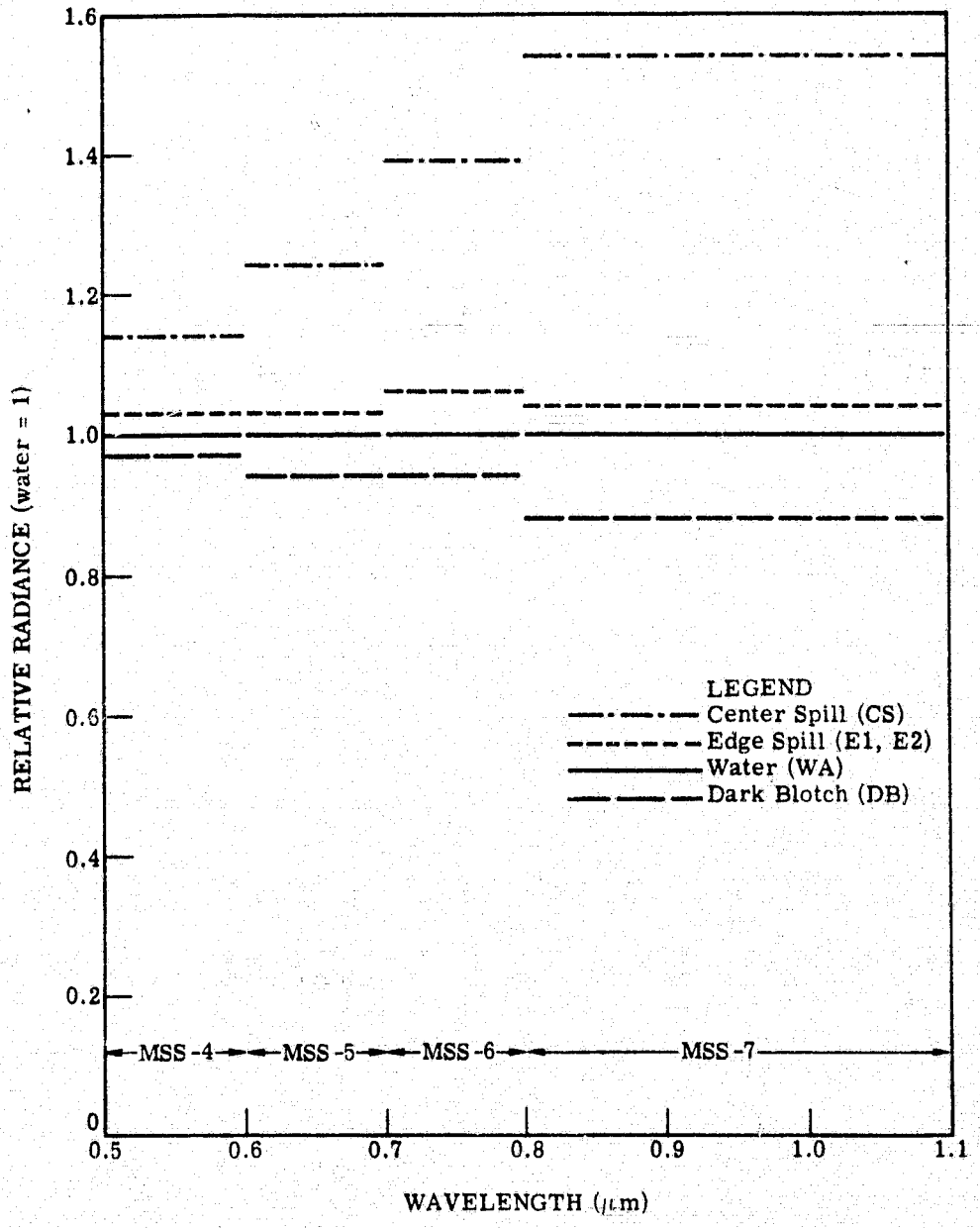

FIGURE 4. EXAMPLE OF VISUAL LISTING OF MEAN RADIANCE VALUES FOR THREE TARGET CLASSES RELATIVE TO WATER. From an ERTS-1 study [8].

comparisons can easily be made between the unknown spill and known signature values for other data.

Another product of the spectral signature method is the comparison of the means and standard deviations of the signatures from one channel to another. A visual presentation of such a comparison is shown in Figure 5. This figure is a plot of the mean values of spectral signatures from one channel versus the mean values from a second channel. The error bands signify the values of the standard deviations. It can be seen from such a display how close or far apart the different signatures are from each other for each of the classes. Therefore, some insight is given into a better description of the material and possibly the total number of signatures required for that description. The correlation between any two channels can be quickly assessed by this method also.

4.2 METHOD OF RADIANCE RATIOS

It was shown by Yarger [9] and others that some quantitative assessment of the degree of the turbidity of the water can be made by computing the ratios of the radiance of two or more spectral channels.

From parametric curves such as Ramsey's [10], it can be seen that the values of radiance in the region from 0.56-0.60 μm (Channel A) and 0.65-0.69 μm (Channel B) would both increase as the amount of floating algae near the surface of the water increased. However, the ratio of the radiance, Channel A/Channel B would always be greater than unity if the algae were the dominant reflecting material at or near the surface of the water. For the case of suspended inorganic material, such as clay and silt, we refer to references such as Polcyn and Rollin [11], which show that as the turbidity increases the

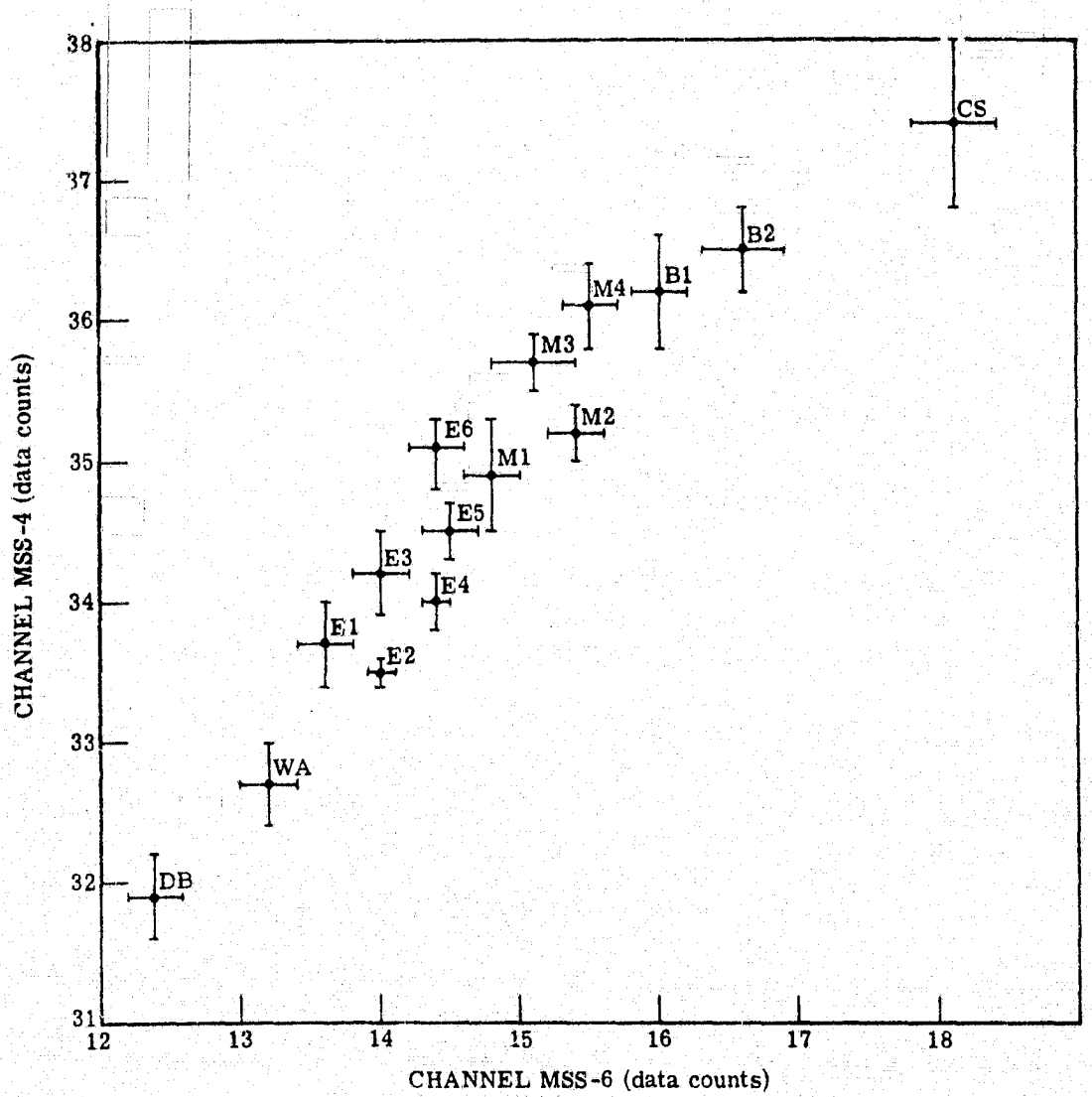

FIGURE 5. EXAMPLE OF COMPARISON OF SPECTRAL SIGNATURES FOR TWO CHANNELS. For the target classes from an ERTS-1 study [8].

reflectance increases in these channels. However, the reflectivity of the short wavelength channels is much lower than that of the longer wavelength channels, and as in our example above, the ratio Channel A/ Channel B would be less than unity.

In the case of oil on the surface of the water, oil has a reflectivity that has about the same spectral shape as that of water. In this case the ratio of the two above channels would be nearly unity.

It must be pointed out that in using this method it is assumed that the ratios are computed using radiance values, not data counts. Also the background radiance level of water has been subtracted from all values, so that only the difference between the foreign material and water is being evaluated.

5
CONCLUSIONS AND RECOMMENDATIONS

This chapter discusses the usability of Skylab as an oil-pollution detector and monitor, and the usefulness of any satellite for such a purpose. It also presents recommendations concerning the minimum accpetable requirements for such a system.

5.1 USABILITY OF SKYLAB AS AN OIL-POLLUTION DETECTOR AND MONITOR

This report has discussed the attempted use of Skylab's photographic and multispectral-scanner systems for detecting and monitoring oil spills on the water. It has gone into some of the theory of oil-pollution monitoring by satellite and described the procedures and results of the evaluation of spills. It was not possible to make an affirmative statement that there was oil present on the water at any time under Skylab.

Many factors were involved in the lack of such a statement. Although the path of the satellite was known before flight, its probability of passing over an active spill site was very low, unless a planned spill were made. The frequency of re-coverage of any given area was also very low, eliminating the testing of the satellite's monitoring capabilities. Also, in spite of the numerous, relatively narrow spectral channels, the noise limitations of the data, and the absence of any data for some of the channels, made analysis virtually impossible. Finally, the time delay in receiving the data prohibited speedy follow-up, if such action had been necessary.

It is difficult, therefore, to say that Skylab would have been useful as an operational detector or monitor of oil spills.

5.2 USE OF ANY SATELLITE AS A DETECTOR OR MONITOR OF OIL POLLUTION

Although much of the previous discussion appears pessimistic, the results of this study and others [3,4,5,8] indicate that in many ways it is both feasible and valuable to use a satellite as a detector and/or monitor of oil spills, in conjunction with other current methods. The advantages of using a satellite-assisted warning and monitoring system are that the satellite can look from an elevated position without ground or structural hinderances (it will, however, be affected by atmospheric conditions), it can maintain its vigil day and night, and it may have built-in alarms to warn if a spill should occur. Furthermore, it can assist in locating the offender, and it can monitor the progress of a spill through its motion, size change, and clean-up.

To accomplish the detection goal, however, it is imperative that the satellite often observe the areas most likely to be affected. This frequency should not be longer than 24 hours, and might be less in more susceptible locations. To further enhance the capabilities of such a system, the number of spectral channels would have to be large to allow for better discrimination of effects due to oil from those of suspended organic and inorganic matter [9,10,11,12,13,14]. The bandwidths should be no wider than 0.05-0.07 μm in the visible region of the spectrum. An example of such an array of channels is 0.47-0.52, 0.53-0.57, 0.56-0.60, and 0.65-0.69 μm [12]. Furthermore, the minimum detectable change in reflectivity (including effects of the atmosphere, the optics and electronics) should be no greater than 1%. Thus, the small changes in the surface of the water resulting from the presence of oil could be seen and separated from natural changes in the water quality. Other band requirements would

include a thermal capability to evaluate the change in thermal emissivity and/or temperature of the surface caused by the presence of the foreign material. This thermal system should have a minimum detectable difference of 1°C or less [2,3,5,12]. The thermal capability would allow observations during the night and aid in identification during the day. High-resolution photography is also very useful, to give the ground observer a fast overview of the area.

Another necessity to make the satellite a feasible asset in an oil monitoring and detecting program is a quick information and data-retrieval system. A time lag of more than a few hours is probably not acceptable. High-speed retrieval will allow for quick analysis, which in turn will result in fast corrective measures taken on the ground.

Finally, it is necessary that the noise limits of the scanner system be low enough to detect the presence of oil on the water surface.

These requirements appear to indicate that a stationary satellite such as the proposed Synchronous Earth Observatory Satellite [12] may be useful. Such a satellite would meet all or most of these requirements and thus could be used to detect and monitor oil spilled on the water in time to prevent serious environmental damage. It could also assist in monitoring clean-up operations, and finally it could greatly assist in law enforcement both by possibly observing the offender in the act, and also by prevention of spills due to an oil industry-wide knowledge of the continuous surveillance.

Even with the technical specifications indicated above, however, two major operational limitations would still exist. First, detection would be limited to rather large spills. Second, the detection of oil slicks very near shore, or in narrow rivers or small estuaries would still be of debatable feasibility. Therefore, operational ability

would be limited to only a small percentage of the oil-pollution incidents presently occurring. However, as the growth of super-tanker traffic and offshore drilling continues, that percentage may change significantly. In addition, while tanker accidents or offshore well blow-outs are relatively infrequent, they can be extremely disasterous when they do occur. Timely monitoring, especially in areas remote from the present system of conventional monitoring activity, could be of great utility.

APPENDIX A

S192 MULTISPECTRAL SCANNER WITH THE X-5 ARRAY OF SENSORS: BACKGROUND

The S192 multispectral scanner was flown and operated in the Skylab space station during the second half of 1973 and the first two months of 1973. The scanner was developed on a very tight schedule, and in order to meet tne performance requirements developmental mercury-cadmium-telluride detectors were employed for the twelve visible/near-IR bands. Although the best of these detectors met the sensitivity requriements, they proved to be unacceptably non-linear. At the expense of some loss in sensitivity this non-linearity was reduced by using optical bias (i.e., constant background illumination). In this way the non-linearity in the response was made manageable but the frequency response still varied somewhat as a function of signal level, as was expected.

To optimize the frequency response in each spectral band, correction circuits were included in the preamplifiers. These circuits were provided with trim-pots for final optimization. This was done with the detector-preamplifier assembly installed in the S192 scanner, by using the trim-pots to optimize the shape of the output signal when a low frequency square wave was inserted optically at the S192 entrance aperture. The resulting signals were not perfect, but analysis of flight data showed that for normal signal levels the residual ringing was comparable to the noise in amplitude and died out rather quickly. As a result the ringing was not noticeable in data presented either as imagery or as A-traces.

During development of the S192 and partly as a result of the concern over the visible/near-IR bands, the single thermal band was not tested as thoroughly as the others. (The thermal detector is mounted in the same dewar as the array of visible/near-IR detectors but uses a separate window.) Linearity was not a problem with this detector, but analysis of flight data showed that its sensitivity (NEΔT $\simeq$ 2.5K) was disappointing.

It was, therefore, decided to resupply the S192 with a new detector-preamplifier package with a better thermal detector. Such a package, with the best obtainable thermal detector, was prepared in some haste and carried to Skylab by the SL4 astronauts. As it was known that the visible/near-IR array of this package, the X-5, was of relatively poor sensitivity, it was not used to replace the original package, the Y-3, except for the final 17 passes of SL4 (passes 84 through 100). SL4 was the final Skylab mission.

Initial analysis of the flight data from the X-5 array confirmed that the thermal channel was much improved (NEΔT ~ 1 K), but this improvement was obtained at the cost of good quality visible and near-IR data.

The reason behind the poor quality of the visible and near-IR data lies in the fact that the X-5 detectors for these channels had nigh-frequency electrical performances different from those of the earlier arrays: the X-5 had better performance in this regard. Since the preamplifiers for each detector had been adjusted to compensate for the poor frequency response of the earlier detector arrays, a substantial overshoot and/or undershoot with the X-5 array occurred every time a substantial change in the input signal occurred.

Therefore, the following S192 spectral channels were subsequently found to be unacceptable: SDO-1, 2, 18, and 22. SDO-5, 6, and 17 are also not available because their detector array elements were not operating during the time of data collection.

Because of this decreasing sensitivity, the noise component of the output of the remaining X-5 sensors was significantly increased. Therefore, when the average scene signal is slightly greater than zero radiance, as in the case of near-IR data over water, the signal will often bounce above and below zero. One of the aspects of the data preparation for users is to eliminate all data values less than zero, and define them as zero. Because of the above reasons this occurred more often than normal, and much of the data as received was not usable.

APPENDIX B

COINCIDENCE OF MAJOR SPILLS AND SKYLAB OVERFLIGHTS

Location	Oil Type	Quantity (Gal.)	Report Date	Clean Date	Skylab Comments
Providence, Rhode Island	#6 Fuel Oil	50,000	12 Apr. 1973	Before 20 Apr. 1973	No Flights
Norfolk, Virginia	Navy Distillate	30,000	27 Apr. 1973	?	No Flights
Grand Isle, Louisiana	Crude	240,000	11 May 1973	15 May 1973	No Flights
Atchafalaya River Morgan City, Louisiana	Crude	63,000	31 May 1973	?	No Overpass
Monangahela River Duquesne, Pennsylvania	#6 Fuel Oil	40,000	1 Jun. 1973	14 Jun. 1973	No Overpass
New York Harbor (M/V Exxon Brussels)	Crude	<80,000	2 Jun. 1973	Before 21 Jun. 1973	No Overpass
Santa Barbara Channel (Coal Oil Point)	Crude	Unknown Seeping	5 Jun. 1973	?	No Overpass
Oakland, California	Bunker C	5,000	5 Jun. 1973	6 Jun. 1973	No Overpass
Atlantic Ocean (37°30'N 74°30'E)	?	?	?	?	No Flights
Rouge River Detroit	4 Oil and Kerosine	20,000	28 Jun. 1973	9 Jul. 1973	No Flights
Savannah River Savannah, Georgia	Tallow	29,800	6 Jul. 1973	10 Jul. 1973	No Flights
Northport, Long Island	#6 Oil	5,000	9 Jul. 1973	10 Jul. 1973	No Flights
Mississippi River Mile 88	Crude	210,000	11 Jul. 1973	12 Jul. 1973	No Flights
Tennessee River Mile 446	#2 Diesel Fuel	15,000	18 Jul. 1973	19 Jul. 1973	No Flights

Location	Oil Type	Quantity (Gal.)	Report Date	Clean Date	Skylab Comments
Lake Michigan Chicago, Illinois	Unknown	"major"	18 Jul. 1973	18 Jul. 1973	No Flights
Ohio River, Mile 894	Gasoline	84,000	7 Aug. 1973	7 Aug. 1973	No Flight
Oakland, California Outer Harbor	Diesel Fuel	3,500	6 Sep. 1973	7 Sep. 1973	No Overpass
Portland, Oregon	Bunker	40-75,000	6 Sep. 1973	90% by 12 Sep. 1973	No Overpass
Houston, Texas	Marine Crude	40-160,000	9 Sep. 1973	11 Sep. 1973	No Overpass
Mississippi River 85 Mi. AHOP	Crude	1,500	9 Sep. 1973	14 Sep. 1973	No Overpass
Norfolk, Virginia	-	1,500	14 Sep. 1973	-	17 Sep. 1973 too late
Vancouver, British Columbia	-	100,000	25 Sep. 1973	After 27 Sep. 1973	No Flights
San Francisco Bay	Fuel Oil	2,000	27 Sep. 1973	2 Oct. 1973	No Flights
Columbus, Georgia Chattahoochee River	Gasoline	8,100	5 Oct 1973	-	No Flights
Gulf of Mexico (28°20'N 93°29'W)	Diesel Fuel	-	12 Oct. 1973	-	No Flights
Enid, Oklahoma Cimarron River	Crude	250,000	15 Oct. 1973	after 23 Oct. 1973	No Flights
Bronx, New York East River	-	80,000	16 Oct. 1973	19 Oct. 1973	No Flights
Albany, New York Hudson River	#6	20,000	19 Oct. 1973	23 Oct. 1973	No Flights
Vancouver, British Columbia	Bunker C	3,000	26 Oct. 1973	28 Oct. 1973	No Flights
Padilla Bay, Washington	Diesel Fuel	-	12 Nov. 1973	-	No Flights

Location	Oil Type	Quantity (Gal.)	Report Date	Clean Date	Skylab Comments
Pittsburgh, Pennsylvania	#2	5,000	12 Nov. 1973	14 Nov. 1973	No Flights
Atlantic Coast (35°20'N 75°05'W)	Diesel Fuel	6,000	12 Nov. 1973	15 Nov. 1973	No Flights
Cincinnati, Ohio Ohio River	-	130,000	1 Dec. 1973	7 Dec. 1973	No Overpass
Seattle, Washington	UP-4	15,000	3 Dec. 1973	7 Dec. 1973	No Overpass
St. Francisville, Louisiana Mississippi, River	Fuel Oil	16,000	5 Dec. 1973	-	No Overpass
Elk River, Minnesota Mississippi River	#4 Fuel Oil	40,000	11 Dec. 1973	-	No Overpass
Cape Cod Canal	Fuel Oil	300,000	21 Dec. 1973	-	No Overpass
Sabine, Texas	Gulf Crude	63,000	22 Dec. 1973	25 Dec. 1974	No Overpass
Houston, Texas	Light Crude	84,000	23 Dec. 1973	After 25 Dec. 1973	No Overpass
Philadelphia Pennsylvania Delaware River	Nigerian Crude	4,000-126,000	26 Dec. 1973	28 Dec. 1973	No Overpass
Mississippi River Mile 20	Gasoline	5,000	28 Dec. 1973	-	No Overpass
Pacific Ocean S. of Monterey California	Bunker C	16,000	29 Dec. 1973	12 Jan. 1974	No Overpass
Trenton, New Jersey Delaware River	#2	20,000	3 Jan. 1974	14 Jan. 1974	No Overpass

Location	Oil Type	Quantity (Gal.)	Report Date	Clean Date	Skylab Comments
Estherville, Kansas Desmoines River	#1	2,000	15 Jan 1974	16 Jan. 1974	No Overpass
New Orleans Harbor	-	630,000	15 Jan. 1974	24 Jan. 1974	No Overpass
Krotz Springs, Louisiana Atchafalaya River	Crude	546,000	16 Jan. 1974	17 Jan. 1974	No Overpass
Mississippi River 1.5 mil AHOP	Gasoline NR 2 Jet Fuel	2,800,000 2,600,000 672,000	18 Jan. 1974	-	No Overpass
Chicago, Illinois San and Ship Canal	#4	2,000	22 Jan. 1974	24 Jan. 1974	No Overpass
Ft. Walton, Destin, Florida	Bunker C	1,000	30 Jan. 1974	31 Jan. 1974	31 Jan 1974 - Too Late
Northville, New York Long Island Sound	-	10,000-20,000	31 Jan. 1974	1 Feb. 1974	No Overpass
Bear Mountain Park Hudson River, New York	Fuel Oil	20,000	11 Feb. 1974	25 Feb. 1974	No Flight
Paulsburo, Ner Jersey	Bunker	285,000	19 Feb. 1974	25 Feb. 1974	No Flight
Norwich, Connecticut	#2	42,000	21 Feb. 1974	After 22 Feb. 1974	No Flight
Milwaukee, Wisconsin Menomenee River	#2 Diesel Fuel	3,000	21 Feb. 1974	After 25 Feb. 1974	No Flight

REFERENCES

1. R. Horvath, W.L. Morgan, and R. Spellicy, Measurements Program for Oil-Slick Characteristics, Report No. 2766-5-P, Willow Run Laboratories, Ann Arbor, Michigan, 1970. Contract DOT-CG-92580-A, USCG.

2. R. Horvath, Interpretation Manual for the Airborne Remote Sensor System, Report of Contract DOT-CG-33568A, Office of Engineering, U.S. Coast Guard, Washington, D.C., January 1974.

3. R. Horvath, W.L. Morgan, and S.R. Stewart, Optical Remote Sensing of Oil Slicks: Signature Analysis and Systems Evaluation, Report of Project No. 724104.2/1, Office of Research and Development, U.S. Coast Guard, Washington, D.C., October 1971.

4. J. Millard and J. Arvesen, "Results of Airborne Measurements to Detect Oil Spills by Reflected Sunlight," in Remote Sensing of Southern California Oil Pollution Experiment, Office of Research and Development, U.S. Coast Guard, Washington, D.C., 1971, pp. 38-62.

5. R. Horvath and S.R. Stewart, "Analysis of Multispectral Data from the California Oil Experiment of October 1971," in Remote Sensing of Southern California Oil Pollution Experiment, Office of Research and Development, U.S. Coast Guard, Washington, D.C., 1971, pp. 91-106.

6. SKYLAB Program Earth Resources Experiment Package Sensor Performance Evaluation, Final Report, Volume II (S-192), MSC-05546, Johnson Space Center, NASA, Houston, Texas, May 1975.

7. End Item Specification for Multispectral Scanner: SCN 020, MSC-TF-192-111, Manned Spacecraft Center, NASA, Houston, Texas, August 1971, p. 9.

8. G. Goldman and R. Horvath, Oil Pollution Detection and Monitoring from Space Using ERTS-1, Report No. 193300-68-F, Environmental Research Institute of Michigan, Ann Arbor, Michigan, July 1975.

9. H.L. Yarger, et al., "Quantitative Water Quality with ERTS-1," in Third Earth Resources Technology Satellite Symposium, Volume I, December 1973, pp. 1637-1651.

10. R.C. Ramsey, Study of the Remote Measurement of Ocean Color, Report No. TRW-NASA-1658, TRW Corporation, Los Angeles, California, 1968.

11. F.C. Polcyn and R.A. Rollin, Remote Sensing Techniques for the Location and Measurements of Shallow-Water Features, Report No. 8973-10-F, Willow Run Laboratories, Ann Arbor, Michigan, 1969.

12. G.C. Goldman, et al., Investigation of Transient Earth Resources Phenomena: Continuation Study, Report No. 107400-2-F, Environmental Research Institute of Michigan, Ann Arbor, Michigan, 1974.